Slave spins away from half filling: Cluster mean-field theory of the Hubbard and extended Hubbard models

S. R. Hassan[1,2] and L. de' Medici[3,4]

[1]*Department de Physique, Université de Sherbrooke, Québec, Canada J1K 2R1*
[2]*The Institute of Mathematical Sciences, C.I.T. Campus, Taramani, Chennai 600113, India*
[3]*Laboratoire de Physique des Solides, Université Paris-Sud-CNRS, UMR 8502, F-91405 Orsay Cedex, France*
[4]*Dipartimento di Fisica, Università di Roma "La Sapienza," Piazzale Aldo Moro 2, I-00185 Rome, Italy*

A slave-spin representation of fermion operators has recently been proposed for the half-filled single and multiband Hubbard model. We show that with the addition of a gauge variable, the formalism can be extended to finite doping. We solve the resulting spin problem using the cluster mean-field approximation. This approximation takes short-range correlations into account by exact diagonalization on the cluster, whereas long-range correlations beyond the size of clusters are treated at the mean-field level. In the limit where the cluster has only one site and the interaction strength U is infinite, this approach reduces to the Gutzwiller approximation. There are some qualitative differences when the size of the cluster is finite. We first compute the critical U for the Mott transition as a function of a frustrating nearest-neighbor interaction on lattices relevant for various correlated systems, namely, the cobaltates, the layered organic superconductors and the high-temperature superconductors. For the triangular lattice, we also study the extended Hubbard model with nearest-neighbor repulsion. In addition to a uniform metallic state, we find a $\sqrt{(3)} \times \sqrt{(3)}$ charge density wave in a broad doping regime, including commensurate ones. We find that in the large U limit, intersite Coulomb repulsion V strongly suppresses the single-particle weight of the metallic state.

I. INTRODUCTION

The theoretical description of strongly correlated systems, such as high-temperature superconductivity, heavy fermions, and ultracold atoms in optical lattices, poses major challenges in the field of the condensed matter physics. These are all systems where the strength of the electron-electron interaction is comparable to or greater than the kinetic energy of the electrons, and this makes any theory based on a perturbative expansion around the noninteracting limit at least questionable. The nonperturbative nature of the problems adds extreme difficulty to theoretical tools describing these systems. In recent years, several radically new and reliable nonperturbative approaches to the problem of strong correlations have been developed such as dynamical mean-field theory (DMFT),[1] dynamical cluster approximation,[2] cluster-DMFT (CDMFT),[3] variational cluster approximation (VCA),[4] two-particle self-consistent approach (TPSC);[5] these approaches have led to substantial progress in our understanding of these systems.

Some other nonperturbative semianalytic approaches based on the idea of slave-variable representations of correlated fermions have also been devised and have been used for decades now, in order to perform nontrivial approximations on many-body models. In this respect, slave bosons have been particularly successful. Their formulation in the limit of infinite correlation strength between the electrons[6] can be systematically introduced as a saddle point approximation plus corrections, and has lead to much insight in the physics of the strongly correlated systems, most notably of heavy fermions. The alternative formulation that can treat finite interaction strength[7] cannot be controlled as a saddle point, but it turns out to be a very practical implementation of the Gutzwiller approximation. It has been generalized to many-orbital models[8] and succeeded in capturing the essential of quasiparticle physics stemming out from the competition between interactions and delocalization energy. High-energy features can be also studied from fluctuations around this mean field.

The main limitation of this last formulation is the fact that the number of slave-variables increases exponentially with the number of degrees of freedom in the mean field, making multiorbital or cluster mean field quickly intractable.

A different approximation, based on quantum rotors as slave variables[9] has been devised, that is much more economical since it introduces only one slave variable per site, dual to the total on-site charge. Still, this technique can only be used correctly at half-filling and cannot address orbital-dependent observables or magnetic properties of the system. It has been nevertheless successfully applied to cluster mean fields, recently.[10] Also an extension of this technique controlled by large degeneracy limits has revealed itself very powerful as an impurity solver.[11]

Recently, a representation of fermion operators that instead uses quantum spins as slave variables has been successfully used to study the multiband Hubbard model at half-filling.[12] In this paper, we generalize this representation away from half-filling and apply it to the study of the Mott transition on the different lattices and the charge density wave (CDW) transition on the triangular lattice. The Hubbard model plays the role of a standard model for correlated fermions on a lattice; it contains the band kinetic energy and the local on-site interaction. In order to study the possibility of a CDW phase, the Hubbard model was extended to include an intersite electron-electron interaction (V). This leads to the so called extended Hubbard model (EHM). This model

has been studied within the DMFT at half[13] and quarter[14] fillings and it is relevant to materials with a charge-ordered phase.[15–17] The problem of the transition between a Mott insulator (MI), a band insulator (BI) with CDW, and a Fermi liquid in this model has been studied in Ref. [18] using extended DMFT.[19] More recently, EHM and its variant on the triangular lattice have been extensively studied in the context of cobaltates.[20–27]

The Hamiltonian for the extended Hubbard model on a two dimensional lattice with sites labeled by i is

$$H = \sum_{\langle ij \rangle \sigma} -t(d_{i\sigma}^\dagger d_{j\sigma} + \text{H.c.}) - \mu \sum_i n_i + \frac{U}{2} \sum_i (n_i - 1)^2$$
$$+ V \sum_{\langle ij \rangle} (n_i - 1)(n_j - 1), \qquad (1.1)$$

where μ, t, U and V are the chemical potential, the nearest-neighbor hopping amplitude, the on-site interaction and nearest-neighbor interaction, respectively, $d_{i\sigma}(d_{i\sigma}^\dagger)$ destroys (creates) an electron on site i with spin σ, $\langle i,j \rangle$ denotes that the sum is over nearest neighbors only and the number operator is $n_i \equiv \sum_\sigma d_{i\sigma}^\dagger d_{i\sigma}$.

In order to treat this problem in the simplest approximation that is capable to yield insight on the physics of short-range correlations, we employ a cluster mean-field approximation (CMFA) based on the slave-spin representation. We have recently shown that cluster mean-field approximation for bosons successfully describe the supersolid phase and phase diagram of bosons on the triangular lattice.[28]

In the following section, we introduce the method. In particular, we introduce the gauge needed to its extension off half-filled regimes. Sec. III presents the results on the Hubbard model, and Sec. IV those on the extended Hubbard model. We then summarize and conclude. The appendices contain various technical details such as the choice of the gauge and the infinite U limit.

II. SLAVE-SPIN MEAN-FIELD THEORY

Slave-spin mean-field theory[12] is the ideal bridge between the slave-variable techniques mentioned in the introduction, when taken at the mean-field level, in that it provides full insight in multiorbital and cluster cases, but still remains the most economical way to do this, since it introduces only one slave variable (a spin-1/2) for every degree of freedom in the mean-field cluster. In practice, for a single-site mean field of a one-band model, two slave-spins (one for spin-up electrons and one for spin-down electrons) are used, whereas for an N-orbital local mean-field or a N-site cluster mean-field of a one-band model the number raises only to $2N$. Each slave spin increases the size of the Hilbert space by a factor of two. The gain is thus enormous compared with slave-boson representations because the number of bosons there grows exponentially with N. Where detailed comparison has been performed one finds, as discussed below in Sec. II C, that the slave-spin mean-field reproduces the results of the Gutzwiller approximation, even if a precise mapping has not yet been rigorously derived.

A. Slave-spin representation for arbitrary filling

In the slave-spin representation, we map the original local Hilbert space of the problem onto a larger local Hilbert space that contains as many fermionic degrees of freedom (named $f_{i\sigma}$) as the original plus the same number of spin-1/2 quantum variables, one for each $f_{i\sigma}$.[29] We then associate to every state of the original physical space one of the states in this larger space by using the correspondence:

$$|n_{i\sigma}^d = 1\rangle \Leftrightarrow |n_{i\sigma}^f = 1, \; S_{i\sigma}^z = +1/2\rangle, \qquad (2.1)$$

$$|n_{i\sigma}^d = 0\rangle \Leftrightarrow |n_{i\sigma}^f = 0, \; S_{i\sigma}^z = -1/2\rangle. \qquad (2.2)$$

In words, when a local orbital and spin state is occupied then the corresponding slave-spin is "up" and if it is empty the slave-spin is "down." With these one-particle local states one construct the many-particle states as usual.

The enlarged local Hilbert space contains also unphysical states such as $|n_{i\sigma}^f = 0, \; S_{i\sigma}^z = +1/2\rangle$ and $|n_{i\sigma}^f = 1, \; S_{i\sigma}^z = -1/2\rangle$. These unphysical states are excluded if the following local constraint is enforced at each site and for each σ:

$$f_{i\sigma}^\dagger f_{i\sigma} = S_{i\sigma}^z + \frac{1}{2}. \qquad (2.3)$$

We then have to map the physical operators onto operators that act in the enlarged Hilbert space. The electron number operator is easily represented by the auxiliary fermions number, i.e., $n_{i\sigma}^d = n_{i\sigma}^f$, but also by the z component of the slave-spin $n_{i\sigma}^d = S_{i\sigma}^z + 1/2$, thanks to the constraint. This allows us to rewrite the density-density interaction terms in the Hamiltonian in terms of the spins only,

$$H_{int} = \frac{U}{2} \sum_i \left(\sum_\sigma S_{i\sigma}^z \right)^2 + V \sum_{\langle i,j \rangle} \left(\sum_\sigma S_{i\sigma}^z \right) \left(\sum_\sigma S_{j\sigma}^z \right). \qquad (2.4)$$

For the nondiagonal operators we generalize the prescription of Ref. [12], i.e.,

$$d_{i\sigma} = f_{i\sigma} 2 S_{i\sigma}^x, \quad d_{i\sigma}^\dagger = f_{i\sigma}^\dagger 2 S_{i\sigma}^x, \qquad (2.5)$$

(where $f_{i\sigma}$ is the auxiliary fermion annihilation operator) to the more general one

$$d_{i\sigma} = f_{i\sigma} O_{i\sigma}, \quad d_{i\sigma}^\dagger = f_{i\sigma}^\dagger O_{i\sigma}^\dagger, \qquad (2.6)$$

in which $O_{i\sigma}$ is a generic spin-1/2 operator, i.e., a 2×2 complex matrix.

It is easy to determine that the most general form for $O_{i\sigma}$ is

$$O_{i\sigma} = \begin{pmatrix} 0 & c_{i\sigma} \\ 1 & 0 \end{pmatrix}, \qquad (2.7)$$

where $c_{i\sigma}$ is an arbitrary complex number, in order for the operator Eq. (2.6) to have, in the physical states of the enlarged Hilbert space, the same effect as the fermionic operators in the original Hilbert space, i.e.,

$$d_{i\sigma}|n_{i\sigma}^d = 0\rangle = 0, \quad d_{i\sigma}|n_{i\sigma}^d = 1\rangle = |n_{i\sigma}^d = 0\rangle,$$

$$d_{i\sigma}^\dagger|n_{i\sigma}^d = 1\rangle = 0, \quad d_{i\sigma}^\dagger|n_{i\sigma}^d = 0\rangle = |n_{i\sigma}^d = 1\rangle. \qquad (2.8)$$

Indeed the two conditions on the left hand side are assured by the fermionic operators $f_{i\sigma}$, i.e.,

$$f_{i\sigma}O_{i\sigma}|n_{i\sigma}^f = 0, \; S_{i\sigma}^z = -1/2\rangle = 0, \quad (2.9)$$

$$f_{i\sigma}^\dagger O_{i\sigma}^\dagger|n_{i\sigma}^f = 1, \; S_{i\sigma}^z = +1/2\rangle = 0, \quad (2.10)$$

for any $O_{i\sigma}$.

The other two conditions instead determine three out of four elements of $O_{i\sigma}$.

$$f_{i\sigma}^\dagger O_{i\sigma}^\dagger|n_{i\sigma}^f = 0, \; S_{i\sigma}^z = -1/2\rangle = |n_{i\sigma}^f = 1, \; S_{i\sigma}^z = +1/2\rangle, \quad (2.11)$$

$$f_{i\sigma}O_{i\sigma}|n_{i\sigma}^f = 1, \; S_{i\sigma}^z = +1/2\rangle = |n_{i\sigma}^f = 0, \; S_{i\sigma}^z = -1/2\rangle, \quad (2.12)$$

imply

$$O_{i\sigma}^\dagger|S_{i\sigma}^z = -1/2\rangle = |S_{i\sigma}^z = +1/2\rangle, \quad (2.13)$$

$$O_{i\sigma}|S_{i\sigma}^z = +1/2\rangle = |S_{i\sigma}^z = -1/2\rangle, \quad (2.14)$$

which impose $O_{i\sigma;11} = 0$, $O_{i\sigma;21} = 1$, and $O_{i\sigma;22}^* = 0$. $O_{i\sigma;12} = c_{i\sigma}$ remains undetermined.

The arbitrariness of the complex number $c_{i\sigma}$ is a gauge of our formulation and stems out from the fact that different operators can have the same effect in the physical subspace of the enlarged Hilbert space, while acting differently on the unphysical states.[30] This difference does not have any effect as long as the constraint is treated exactly. In practice, the local constraints are enforced via Lagrange multipliers and approximations have to be performed on these and on the Hamiltonian in order to solve the model. In these approximations, the particular choice of the gauge comes into play. $c_{i\sigma}$ can indeed be tuned in order to give rise to the most physical approximation scheme, by imposing, for instance, that it correctly reproduces solvable limits of the problem, such as the noninteracting limit. We will see that the correct choice of $c_{i\sigma}$ depends on the average occupation of the local state, and is such that it reduces to 1 at occupation 1/2, so that $O_{i\sigma} = 2S_{i\sigma}^x$ and the prescription Eq. (2.5) used at half-filling in Ref. 12 is correctly recovered.

Finally, in the enlarged Hilbert space the Hamiltonian can be written exactly as:

$$H = -t\sum_{\langle ij\rangle\sigma} O_{i\sigma}^\dagger O_{j\sigma} f_{i\sigma}^\dagger f_{j\sigma} - \mu\sum_{i\sigma} n_{i\sigma}^f + \frac{U}{2}\sum_i \left(\sum_\sigma S_{i\sigma}^z\right)^2$$
$$+ V\sum_{\langle i,j\rangle} \left(\sum_\sigma S_{i\sigma}^z\right)\left(\sum_\sigma S_{j\sigma}^z\right), \quad (2.15)$$

subject to the constraint Eq. (2.3).

B. Mean-field approximation

An approximation is now introduced, which consists in three main steps: (1) treating the constraint on average, using a static and site dependent (but spin independent, since we will not investigate here magnetic phases) Lagrange multiplier λ_i (2) decoupling auxiliary fermions and slave-spin de-

grees of freedom and finally (3) treating the slave-spin Hamiltonian in a CMFA, that takes into account the nearest neighbor correlations induced by V.

After the first two steps, the total Hamiltonian can be written as the sum of the following two effective Hamiltonians:

$$H_f = -t\sum_{\langle i,j\rangle,\sigma} Q_{ij} f_{i\sigma}^\dagger f_{j\sigma} + \text{H.c.} - \sum_i (\mu + \lambda_i) n_i^f, \quad (2.16)$$

$$H_s = -\sum_{\langle ij\rangle,\sigma} J_{ij} O_{i\sigma}^\dagger O_{j\sigma} + \text{H.c.} + \sum_{i,\sigma} \lambda_i\left(S_{i\sigma}^z + \frac{1}{2}\right)$$
$$+ \frac{U}{2}\sum_i \left(\sum_\sigma S_{i\sigma}^z\right)^2 + V\sum_{\langle i,j\rangle} \left(\sum_\sigma S_{i\sigma}^z\right)\left(\sum_\sigma S_{j\sigma}^z\right). \quad (2.17)$$

The parameters Q_{ij} (hopping renormalization factor), J_{ij} (slave-spin exchange constant) and λ_i in these expression are determined from the following coupled self-consistency equations:

$$Q_{ij} = \langle O_{i\sigma}^\dagger O_{j\sigma}\rangle_s, \quad (2.18)$$

$$J_{ij} = t\langle f_{i\sigma}^\dagger f_{j\sigma}\rangle_f, \quad (2.19)$$

$$\langle n_{i\sigma}^f\rangle_f = \langle S_{i\sigma}^z\rangle_s + \frac{1}{2}, \quad (2.20)$$

where $\langle\;\rangle_{f,s}$ indicates the effective Hamiltonian used for the calculation of the averages. We shall denote the nearest-neighbor and next-nearest-neighbor values of Q_{ij} as Q and Q', respectively.

We are thus left with two coupled Hamiltonians: a renormalized free fermion Hamiltonian for the $f_{i\sigma}$ and a lattice Hamiltonian for the slave-spins that retains the full complexity of the original problem. We have thus to perform a further approximation, in this case the cluster mean field, on the spin Hamiltonian.

A cluster with a finite number of sites only is considered, within which interactions are treated exactly, and is embedded in the effective ("Weiss") field of its surroundings. A tiling of the original lattice is made, out of copies of the chosen cluster unit (cluster shapes are chosen to respect lattice symmetry), assuming translational invariance in the superlattice defined by this tiling, and this approximate Hamiltonian is used to calculate the mean-field average values.

In practice, this means that in this approximation an effective Hamiltonian of a finite cluster is enough to represent the physics of the full lattice and that the "Weiss fields" are calculated using this same Hamiltonian (i.e., self-consistently) that represents also the surroundings of the cluster unit and not only the cluster unit itself.

Mathematically, we consider the following Hamiltonian for the slave-spin cluster C:

$$H_s^C = \sum_{\langle ij\rangle\in C} H_s[i,j] + \sum_{i\in C,\sigma} h_{i\sigma} O_{i\sigma}^\dagger + \text{H.c.} + \sum_{i\in C} h_i^z S_i^z, \quad (2.21)$$

where $h_{i\sigma}$ and h_i^z are the effective fields of the surroundings. H_s^C needs to be diagonalized with the following self-consistency condition:

$$h_{i\sigma} = \sum_{jn.n.i}' J_{ij} \langle O_{i\sigma} \rangle, \qquad (2.22)$$

$$h_i^z = \sum_{jn.n.i}' V \langle S_{j\sigma}^z \rangle, \qquad (2.23)$$

where the prime over the sum means that sites j inside the cluster are excluded.

We summarize the iteration scheme we used in order to solve these mean-field equations for a given filling n: (i) start the iteration by guessing the exchange constants J_{ij} and the effective fields $h_{i\sigma}$ and h_i^z, diagonalize the spin Hamiltonian H_s^C iteratively adjusting the λ_i's to satisfy the constraint Eq. (2.20) (ii) calculate the average values in Eq. (2.18) to determine Q_{ij} and those in Eqs. (2.22) and (2.23) to determine the "new" $h_{i\sigma}$ and h_i^z from the Hamiltonian H_s^C (iii) insert the value of Q_{ij} and λ_i in the fermionic Hamiltonian Eq. (2.16), and determine the exchange constant J_{ij} (iv) repeat from the step (i) with the new $h_{i\sigma}$ and h_i^z until all quantities are converged.

It is useful to underline the role of two key quantities, in characterizing the physics of the system. It can be shown that $Z = \langle O_{i\sigma} \rangle^2$ is the quasiparticle weight, while the effective mass enhancement is set by the effective hopping renormalization Q_{ij}. The two quantities coincide if the mean-field approximation on the slave spin Hamiltonian is taken at the single-site level. In that approximation they both vanish in the Mott insulating phase. This amounts to neglecting all number fluctuations within the Mott phase, which is too crude of an approximation especially when close to the Mott transition. On the contrary in the CMFA that we consider here these two quantities are distinct and one can have e.g., a Mott transition where the mass stays finite as we will see in the following. We use Z as an order parameter: $Z \neq 0$ indicates a metallic state, while Mott/CDW insulating behavior corresponds to $Z = 0$.

C. Choice of the gauge $c_{i\sigma}$

We now discuss how to fix the gauge represented by the complex number $c_{i\sigma}$.

The physical condition that we choose to impose is that our CMFA reproduces correctly the noninteracting limit, i.e., when $U = V = 0$,

$$Q_{ij} = Z = 1, \qquad (2.24)$$

for any given filling $n_{i\sigma}^f = n$, so that $c_{i\sigma} = c(n_{i\sigma}^f)$.

In the single-site approximation (whose equations are easily obtained by reducing the cluster C to one site only) $Q_{ij} = Z$ by construction and, thus, $Z = 1$ is the only condition to be enforced. As detailed in Appendix A, $c_{i\sigma}$ can be chosen purely real and it can be determined analytically. It takes the form:

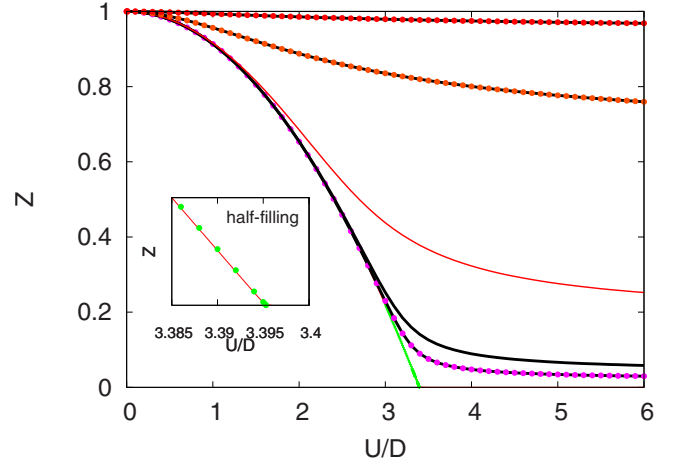$$c = \frac{1}{\sqrt{n(1-n)}} - 1. \qquad (2.25)$$

FIG. 1. (Color online) Comparison of slave-spin [within the gauge Eq. (2.25), continuous lines] and slave-bosons (dots) single-site mean-fields in the one-band Hubbard model. For any fixed population (from below, the filling per spin is $n = 0.5, 0.495, 0.49, 0.45, 0.25, 0.05$) the two methods give coincident results. Inset: blow up of the Mott transition at half-filling, $n = 0.5$.

With this choice we see from Fig. 1 that at the same fixed population n the single-site mean field of the Slave Spins method gives exactly the same results of the Kotliar-Ruckenstein mean-field of the Slave Bosons method, i.e., the Gutzwiller approximation.

More generally, and namely in the cluster mean-field approximation used in this paper, c has to be determined numerically by solving the mean-field equations at $U = V = 0$ and imposing the conditions (2.24), and is a complex number, i.e., $c = |c|e^{i\phi}$ In Fig. 2, we show $|c|$ and ϕ as a function of n^f for a triangular cluster on a triangular lattice, and $|c|$ for the single-site mean-field approximation [in which the lattice geometry is irrelevant, and indeed the numerical result shown matches the generic analytical one Eq. (2.25)].

We note that in both cases at half-filling $|c| = 1$ and $\phi = 0$, and $O_{i\sigma}$ coincides with the form chosen in Ref. 12, as anticipated.
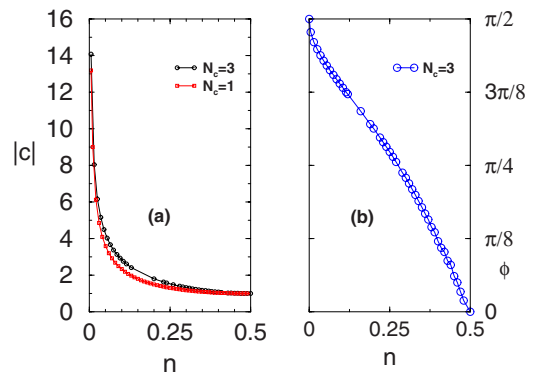

FIG. 2. (Color online) Modulus and phase of the gauge c that determines the choice of the proper hopping operators in the enlarged Hilbert space, in order for the CMFA to reproduce the noninteracting limit. For $N_c = 1$ (single-site approximation) c can be chosen real (that is $\phi = 0$) for all fillings
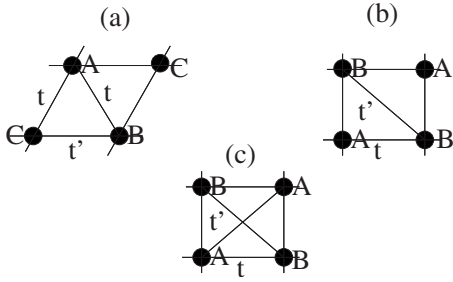
FIG. 3. Illustration of the lattices with hopping amplitude t and t'. (a) $\sqrt{3} \times \sqrt{3}$ sublattice decomposition of the anisotropic triangular lattice (ATL) (b) and (c) two sublattice decomposition of the anisotropic frustrated square lattice (AFSL) and the isotropic frustrated square lattice (IFSL). A, B, and C indicate the sublattice decomposition.

III. HUBBARD MODEL

The Mott transition, i.e., the metal-insulator transition driven by the strength of electron-electron interaction in a homogenous phase, has been studied in great detail using various approaches such as slave bosons, DMFT and its extensions. In this section, we revisit the Mott transition on the lattices shown in Fig. 3. The control parameters are interaction strength U/t and frustration strength t'/t, the ratio of next nearest neighbor to nearest-neighbor hopping amplitude. As a function of these parameter, the Hubbard model at half filling has, within CMFA, four possible phases: a paramagnetic metallic phase, a paramagnetic insulating phase, an insulating antiferromagnetic phase, and (in the presence of frustration) an itinerant antiferromagnetic phase. However, we shall be concerned here with the transition between the paramagnetic metal to paramagnetic insulator. We study the paramagnetic solution by enforcing the spin symmetry, hence, avoiding the opening of a full spectral gap due entirely to magnetic ordering.

The single-site ($N_c=1$) mean-field theory of slave spin representation gives the same results of the Gutzwiller approximation. In this regards CMFA provides a way to go beyond the Gutzwiller approximation.

First, we discuss the Mott transition on the isotropic triangular lattice. To get the uniform phase solution, we enforce the Lagrange multiplier λ_i and the complex number c to be the same for every site within the cluster. In Fig. 4, we plot Z and Q as a function of U at half-filling for cluster sizes $N_c=1,3$. The critical value U/t, at which the Mott insulating phase occurs is 16.2, in the single-site ($N_c=1$) approximation, while it is around 15.1 in the three sites ($N_c=3$) CMFA. The short range correlations, which are built in the CMFA, suppress the critical value U by 6%. The critical value of U obtained from other methods such as DMFT-exact diagonalization (eight site),[31] exact diagonalization calculation for 12 site clusters,[32] and CDMFT[33] are $U_c/t=15$, 12, and 10.5, respectively. In CDMFT the transition is first order.

For $N_c=1$, the slave spin approach is identical to the Gutzwiller approximation,[12] Q and Z are identical and they vanish at the same critical value of U. We show, for $N_c=3$, Q as a function of U. It can be seen that it continues to be nonzero in the Mott insulating phase, and behaves as a t/U,
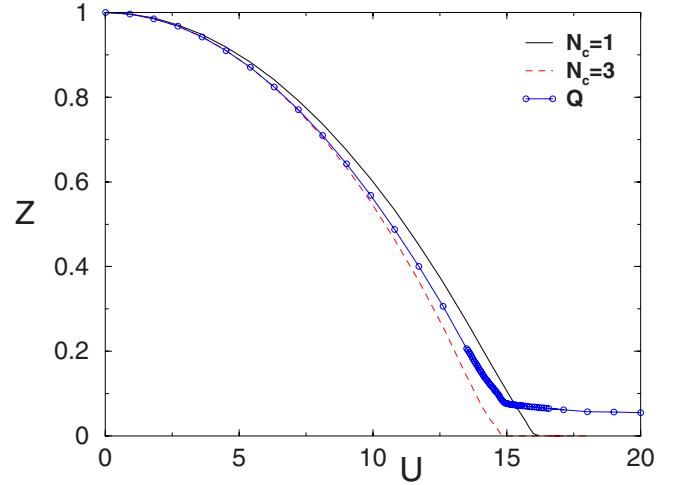

FIG. 4. (Color online) The order parameter Z and the effective hopping Q as function of U for the half-filled Hubbard model. Within CMFA ($N_c=3$) the renormalized hopping Q remains finite in the Mott insulating phase. U is measured in unit of t.

as expected from the fact that the average kinetic energy is nonzero in a Mott insulator.

It should be noted that there is a substantial difference between U_c obtained from 3-site slave-spin CMFA and three-site CDMFT. It is because the dynamical "Weiss-field" of CDMFT captures more accurately the fermionic quantum dynamics compared to our static one.

We now examine Z as a function of doping in the limit $U \to \infty$ since this quantity can be obtained in closed form in the Gutzwiller approximation. We show in Appendix B that for cluster size $N_c=1$, one recovers precisely the Gutzwiller approximation result $Z=2x/(1+x)$, where x is the total doping, $2n=1-x$. In CMFA, we can ask how Z is modified in the presence of short-range correlation effects. It can be seen in Fig. 5 that the short range correlation effect on Z is only appreciable for moderate to large doping x and enhances Z in comparison to the single-site mean field.

We now move on to the dependence of the Mott transition on lattice and frustration. In the absence of magnetic frustra-
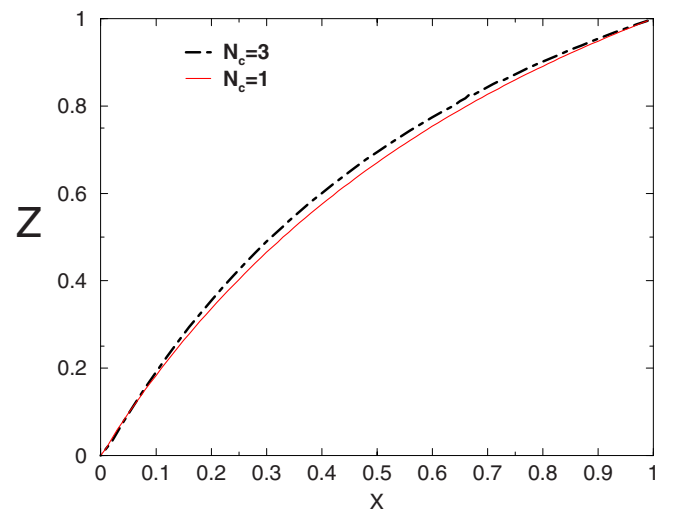

FIG. 5. (Color online) The order parameter Z as a function of doping in the large U limit of the Hubbard model for $N_c=1,3$.
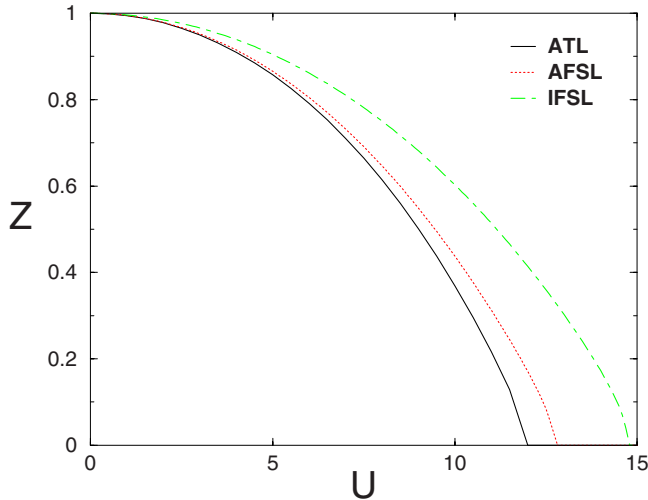
FIG. 6. (Color online) The order parameter Z as function of U at $t'=0.4$ for the lattices ATL, AFSL, and IFSL. U is measured in units of t.

tion on a bipartite lattice, one expects to find an antiferromagnetic ground state at low temperature. Ideally, the Mott transition can occur in systems where antiferromagnetic correlations are frustrated. In the $t-t'$ Hubbard model on the square lattice, a next-nearest-neighbor hopping t' frustrates antiferromagnetic correlations. By studying the lattices shown in Fig. 3, we thus investigate the effects of frustration on the Mott transition in the half-filled $t-t'$ Hubbard model. For $t'=0$ the lattices shown in Fig. 3 correspond to the unfrustrated systems and the effect of the frustration can be systematically studied as t' is increased to its maximal value $t'=t$. Figure 6 displays the order parameter, quasiparticle weight Z as a function of U in presence of sizeable frustration ($t'=0.4$) for various lattices. At this value of t', the critical value U for the Mott transition is the lowest on the anisotropic triangular lattice (ATL), while it is the highest on the isotropic frustrated square lattice (IFSL). As a function of increasing frustration, the critical value of the Mott transition increases as shown in Fig. 7 for the isotropic frustrated square lattice. This increase in t'/t is also seen in the variational cluster approximation.[34] In Fig. 8, we show the nearest and the next-nearest-neighbor effective hopping Q and Q' of auxiliary fermions. It can be seen that deep in the insulating phase they behave as t/U and t'/U, respectively. Nonzero values of Q and Q' in the insulating phase signal that the auxiliary electrons (not the physical electrons) have a Fermi surface (with Luttinger Volume). It also implies, in contrast with infinite dimension (where single-site mean-field theory is exact), that in finite dimension the effective mass does not diverge in the insulating phase, despite the fact that $Z \rightarrow 0$.

Finally, we show in Fig. 9 the phase diagram in $U-t'$ plane for the above mentioned three lattices. One notices that frustration always increases the critical value for the Mott transition and it is particularly effective in the IFSL.

IV. EXTENDED HUBBARD MODEL

We now turn to the study of the extended Hubbard model on the isotropic triangular lattice, since this model has been a
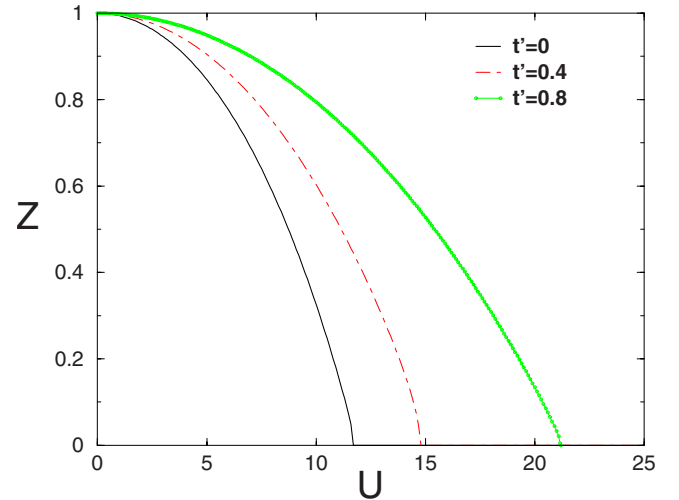
subject of intense investigation in the context of Cobaltates,[20–27] by turning on the nearest-neighbor repulsion V. We will focus on the uniform phase in Sec. IV A, while we will allow charge ordering in Sec. IV B, in order to study the occurrence of a CDW phase.

A. Uniform phase

We first study for different ranges of parameters U, V, and doping x, the uniform phase, by enforcing the Lagrange multipliers to be the same at every site on the cluster and thus avoiding charge ordering. Let us first examine the combined effect of U and V on Z at $x=0$. The uniform ground state phase diagram in the $U-V$ plane that is shown in Fig. 10. For $U<10$ the system is in the metallic state for any values of V. For $10<U<15$, the system enters into the Mott insulating phase upon increasing V. We note however that there

FIG. 7. (Color online) The order parameter Z as a function of U for various values of t' for IFSL. U is measured in units of t.
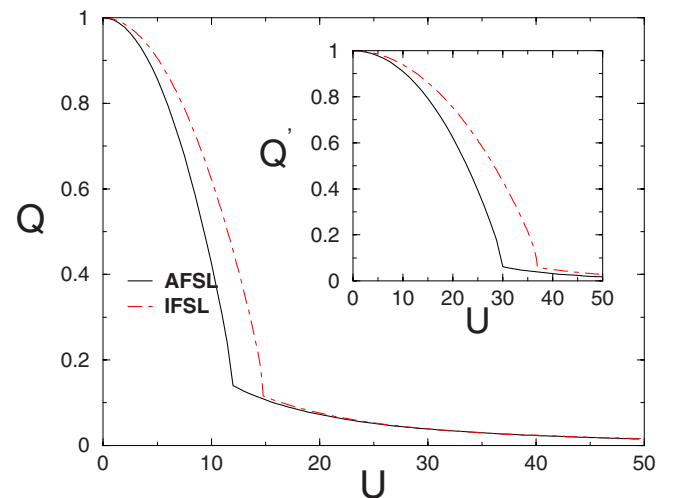

FIG. 8. (Color online) The nearest neighbor effective hopping Q as function of U at $t'=0.4$ for AFSL and IFSL lattices. U is measured in units of t. Inset shows the next-nearest-neighbor effective hopping Q' as a function U in unit of t' at $t=2.5$.
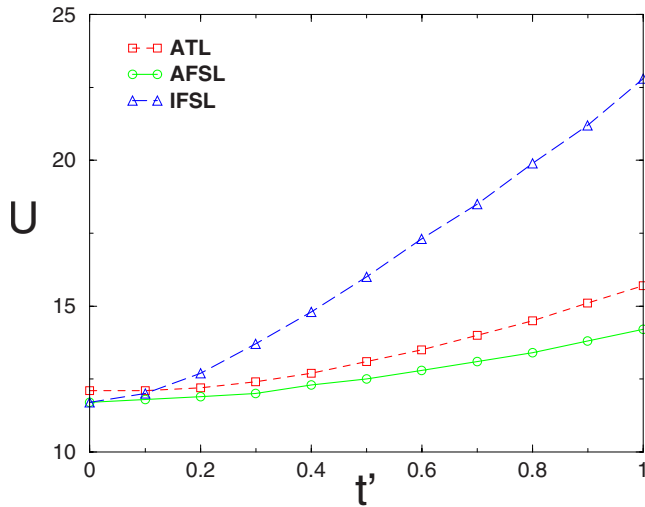
FIG. 9. (Color online) Phase diagram of the Hubbard model on the three lattices considered in this article, as a function of U and t' (in units of t).

is a "reentrant" shape of the phase diagram at larger $U > 15$. For increasing V the system goes from insulating to metallic to Mott-insulating again. This reentrant structure emerges when U and V are comparable. It is because V compensates the effect of U, and moving an electron onto a nearest neighbor to have a doubly occupied site, as in a metallic phase, may become energetically favorable since the repulsion on the nearest-neighbor is comparable to that on-site. The reentrant behavior for V large compared with U and the metallic state for all V and $U < 10$ might well be completely unphysical due purely to the fact that we assume a uniform phase. We test the validity of this phase diagram by allowing CDW instability, which we discuss in a detail in the Sec. IV B.

From the study of sodium cobalt oxide in Ref. 35, it appears that there is a large suppression of the valence-band width—by an order of magnitude compared with the local
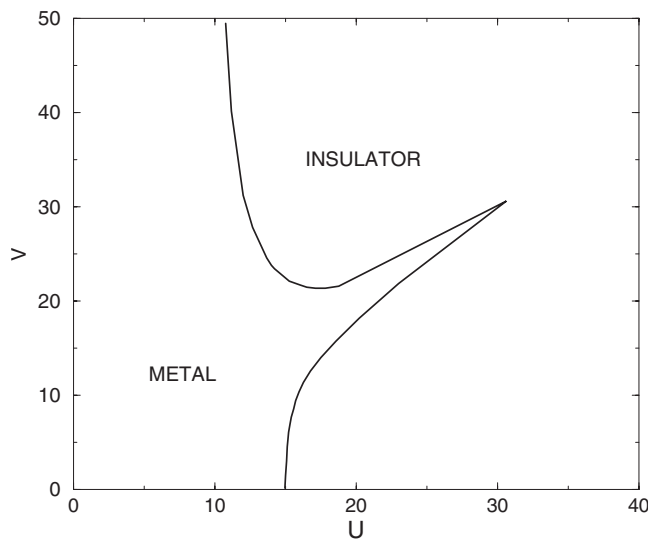

FIG. 10. Phase diagram of the extended Hubbard model on the triangular lattice at half-filling in the uniform phase. U and V are measured in unit of t.
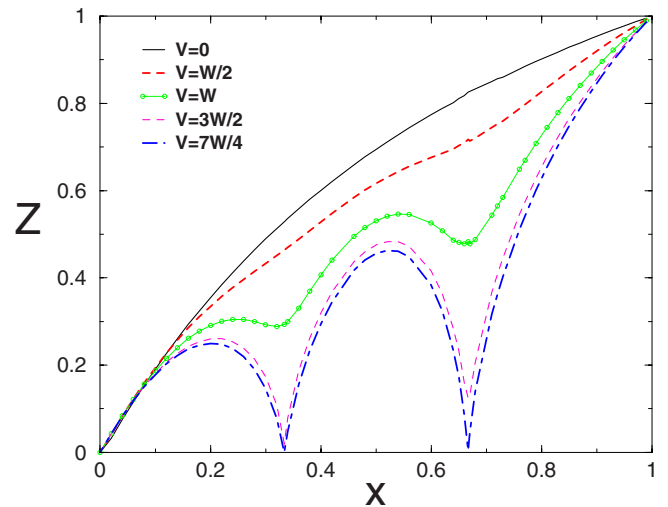

FIG. 11. (Color online) Z as a function of doping x at $U = 100t$ for various values of V. W is the full bandwidth of the isotropic triangular lattice ($W = 9 \ t$).

density approximation (LDA) band structure calculation.[36] Reference 22, based on a study of the Hubbard model on the triangular lattice by means of a Jastrow-Gutzwiller wave-function projection, suggested that such large renormalization of the hopping may be caused by the intersite repulsion V. We confirm these findings by means of our slave-spin CMFA that should be more accurate than the Jastrow-Gutzwiller approximation, because it captures the short-range correlation effect of V in a better way since this term is treated exactly on the cluster.

In Fig. 11, we show Z as a function of x for different values of V at $U = 100$. We choose $U = 100t$ in order to reproduce the $U = \infty$ result of JG study of Ref. 22 It should be noted that Z vanishes at the commensurate dopings $x = 1/3$ and $x = 2/3$ when V is large enough ($V = 7W/4$ in our case, where $W = 9t$ is the full bandwidth of the isotropic triangular lattice). Indeed at doping 2/3 the dominant configurations at large V on any triangle are $(\downarrow, \downarrow, \uparrow)$ $(\downarrow, \uparrow, \downarrow)$ $(\uparrow, \downarrow, \downarrow)$. Now Z involves flipping a spin. So we have to make transition to states like $((\downarrow, \downarrow, \downarrow)$ or $(\uparrow, \uparrow, \downarrow)$ etc. These have a higher energy in the presence of V. Similar arguments holds for at doping 1/3. Z vanishes in our case around $V = 7W/4$, which is a slightly larger value in comparison to the Jastrow-Gutzwiller (JG) study, where it occurs at $V \simeq W$.

The effect of V on the effective hopping tQ is not as strong as we observe on Z (not shown) since on a single triangle, there is no cost to move the particle via a kinetic move, e.g.: $(\downarrow, \downarrow, \uparrow) \rightarrow (\downarrow, \uparrow, \downarrow)$. This is strictly true on a single triangle not connected on anything else, but the mean-fields connected to the triangle will have a small effect, which manifests itself by a small suppression in the effective hopping. For larger clusters, beyond $N_c = 3$ however, it is clear that the effective hopping (and hence the bandwidth) will be further suppressed.

B. CDW instability

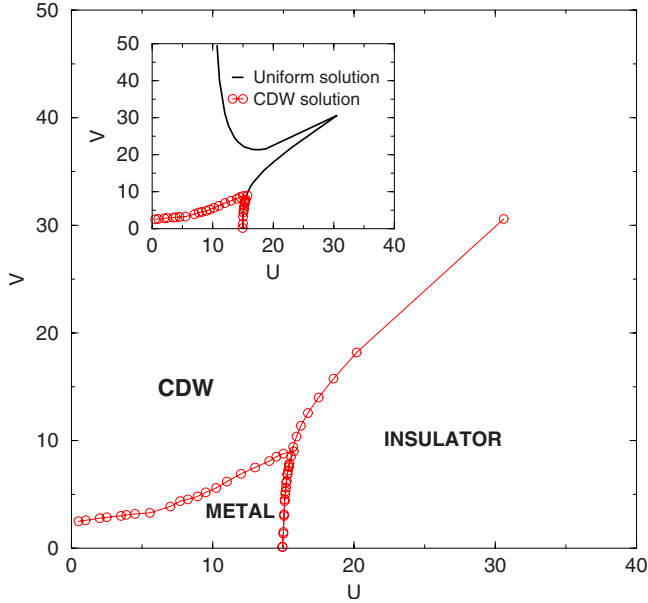It is known, and rather intuitive, that the presence of a nearest-neighbor repulsion in the Hubbard model favors the

FIG. 12. (Color online) Phase diagram in $U-V$ plane for the extended Hubbard model on the triangular lattice at half-filling. The inset shows its comparison with the uniform solution.

tendency toward the formation of charge density waves. In this section, we study the instability of a nonordered phase toward a CDW in the presence of V. We determine for a few dopings the ground-state phase diagram in the $U-V$ plane of the system that has the $\sqrt{3} \times \sqrt{3}$ ordering pattern.

The $\sqrt{3} \times \sqrt{3}$ decomposition of the triangular lattice has been shown in Fig. 3(a), where A, B, and C indicate the sublattice decomposition. We choose cluster size $N_c = 3$, where all three sites A, B, and C within cluster are distinct. In Sec. II, we have discussed how to determine the self-consistent quantities such as, Q, J, h, and h_z. In the present case, we allow the quantities Q_{ij} and J_{ij} to be different for every bond on the cluster, and the quantities $h_{i\sigma}$, h_i^z, λ_i, and the gauge c_i to be site dependent. The complex number c_i is fixed separately for each site in the cluster, using for both the magnitude of the complex number and its phase, the $c(n)$ relation obtained on the uniform noninteracting system.

We solve the mean-field equations and determine the order parameters Z_A, Z_B, and Z_C. When all of them are equal and nonzero one has a metallic phase, while the vanishing of all of them would indicate CDW insulating phase. Unequal Z's, instead, imply a CDW metallic phase.

In the previous section, while discussing the reentrant behavior for V comparable to or larger than U, and the metallic phase for $U < 10$ and $V > 0$, we pointed out that this feature might be unphysical for V larger than U since we do not allow the CDW instability. By allowing the CDW instability, we redo the calculation and find that the uniform phase diagram is not valid for V larger than U. In Fig. 12, we show the phase diagram at half-filling. First, we note that the reentrant feature is missing, rather we find a small window of Mott insulator-metal-CDW transition. Although we have allowed CDW instability, we find that system remains in the uniform phase for high U and low V, and for this range of parameters we find two phases: metallic and Mott insulating. The inset
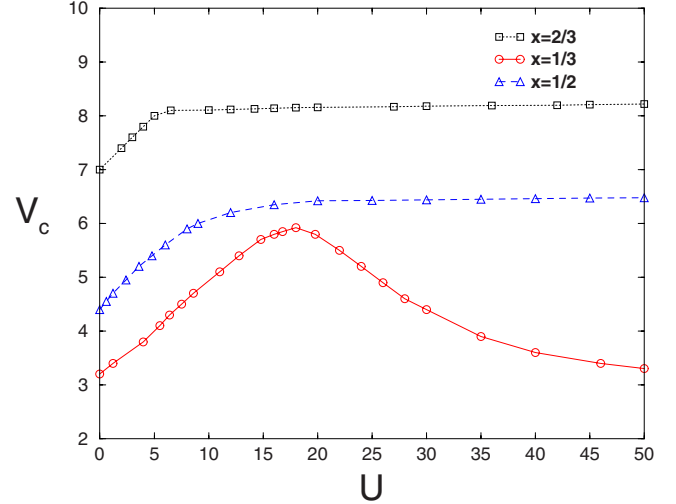

FIG. 13. (Color online) Phase diagram in $U-V$ plane for $x = 1/3, 1/2, 2/3$. The CDW phase is above the lines for the corresponding fillings.

of Fig. 12 displays the comparison of two solution: uniform and CDW. The CDW insulating phase is obtained when V prevails, and the metallic phase when the Kinetic energy overcomes the interaction. In the Mott insulating phase the system can develop an antiferromagnetic long-range order if the magnetic frustration is weak.

This phase diagram is a quite similar to the one of Ref. 18, where it was studied for three–dimensional (3D) extended Hubbard model at finite temperature using extended DMFT, which was viewed as a qualitative representation of the actual phase diagram at $T=0$. It should be noted that our $T=0$ calculation on a two-dimensional-triangular lattice exhibits similar behavior as in the 3D case.

Figure 13 shows the resulting CDW phase diagram in the $U-V$ plane for three special values of doping x. The transition from metallic to CDW phase is first order (at the present level of approximation, we always find a jump in the order parameter Z at the transition point). We also note that the effective mass $1/Q$ diverges at the transition. We note that the lowest value of V_c is at $x=1/3$. We also do not find that dopings $x=1/3$ and $2/3$ are playing any special role, as was suggested in the JG study. It should also be noted that we find the CDW state at $x=0.5$ in contrast with the prediction of the uniform phase in our study (where Z never vanishes) and in the JG study.[22]

The slave-boson mean-field study of Ref. 23 instead predicts a phase diagram similar to ours. However, compared to Ref. 23, our method includes the effect of short-range correlations.

V. CONCLUSION

We have presented an extension of the slave-spin formalism of Ref. 12 away from half-filling by introducing a gauge variable. We have shown how to solve the resulting model in the CMFA in order to go beyond the widely used single-site mean-field. While in the single-site mean-field approximation the gauge variable can be chosen as pure real number, it

is a complex number in the cluster approximation. The advantage of the CMFA method lies in the fact that the short-range correlations can be properly taken into account.

In the single-site approximation for the Hubbard model, we have found analytically that in the infinite U limit our method reproduces the Gutzwiller result. In the CMFA, short-range correlations modify this result. The modifications are more important for intermediate dopings but they are never very large.

We have applied this approach to the Hubbard and to the extended Hubbard model. In the case of the half-filled Hubbard Model, we have revisited the Mott transition on three class of lattices: ATL, high-T_c lattice (ISFL), and organic superconductor lattice (AFSL). We have performed a detailed study of the critical value U_c where the Mott transition occurs as a function of the frustration strength t', and have shown that the effect of t' in the presence of the short range correlations is to increase the critical value for the Mott transition $U_c(t')$.

We have also studied the extended Hubbard model in two dimensions at half filling. We have shown that dopings 1/3 and 2/3 play a special role in the uniform phase. The quasiparticle weight can vanish at these dopings yielding a Mott insulating phase.

For the extended Hubbard model away from half-filling, we have found two ground state phases on the triangular lattice: the metallic and the $\sqrt{3} \times \sqrt{3}$ CDW state in a broad doping regime. At the present level of approximation, we found that, contrary to the uniform phase, dopings 1/3 and 2/3 in the CDW state do not play a special role.

Finally, we point out that this method can be used to study magnetic phases. That has been left for future work. It can also be applied to study the physics of the multiband Hubbard model away from half-filling[37] and can be generalized to tackle the t-J Model, and other strongly correlated models.

ACKNOWLEDGMENTS

APPENDIX A: CHOICE OF THE GAUGE C IN THE SINGLE-SITE MEAN-FIELD

In the single-site approximation, we can determine the gauge c analytically.[38]

The noninteracting single-site slave spin Hamiltonian H_s reads[12]

$$H_s = hO^\dagger + h^*O + \lambda\left(S^z + \frac{1}{2}\right),\qquad\text{(A1)}$$

where O is defined as in Eq. (2.7). The single-site fermionic part of the Hamiltonian is simply spinless noninteracting fer-

mions. The physical spin index σ is suppressed in H_s since for $U=0$ up-spin and down-spin fermions are decoupled, so that we can diagonalize the Hamiltonian for one slave spin in the $S^z = \pm 1/2$ basis. The ground state eigenvalue ϵ_{GS} and the corresponding eigenstate are

$$\epsilon_{GS} = -\sqrt{\frac{\lambda^2}{4} + |a^2|} \equiv -R,\qquad\text{(A2)}$$

$$|GS\rangle = \begin{pmatrix} \dfrac{\frac{\lambda}{2} + R}{N} \\[2mm] \dfrac{-a*}{N} \end{pmatrix},\qquad\text{(A3)}$$

with $N = \sqrt{2R(\frac{\lambda}{2} + R)}$ and $a = h + ch^*$.

The expectation value of S^z and O in the ground state are

$$\langle S_z \rangle = \frac{\lambda}{4R}\qquad\text{(A4)}$$

and

$$\langle O \rangle = -\frac{ca^* + a}{2R}.\qquad\text{(A5)}$$

The Lagrange multiplier depends on the density n and is adjusted in order to satisfy the constraint equation:

$$n - \frac{1}{2} = \langle S_z \rangle = \frac{\lambda}{4R}.\qquad\text{(A6)}$$

We want to tune c in order to match the condition that in the limit $U=0$ the renormalization factor Z must be unity:

$$Z = \langle O \rangle^2 = \frac{|ca^* + a|^2}{4R^2} = 1.\qquad\text{(A7)}$$

We can easily eliminate λ from these two conditions, by squaring Eq. (A6). We are left with the following expression for c:

$$\frac{|a|^2}{|ca^* + a|^2} = n - n^2.\qquad\text{(A8)}$$

If we choose c to be real then h and a are also real. Then, the expression for c in the closed form is

$$c = \frac{1}{\sqrt{n(1-n)}} - 1.\qquad\text{(A9)}$$

Note that this result is independent of h.

This cannot be done in the cluster case, since also the condition $Q=1$ has to be imposed and c has to be chosen complex in order to satisfy this further equation.

APPENDIX B: SLAVE-SPIN FORMULATION OF THE INFINITE-U LIMIT OF THE HUBBARD MODEL

We derive here the analytic expression for Z as a function of doping in the infinite U limit and in the single-site approximation.

In this limit, no double occupancy is allowed so that the interaction term is replaced by a projector that enforces this constraint. In order to do this we replace $O_{i\sigma}$, as defined as in Eq. (2.7), by

$$\widetilde{O}_{i\sigma} = \left(\frac{1}{2} - S^z_{i\bar{\sigma}}\right)O_{i\sigma}, \qquad (B1)$$

where $\bar{\sigma} = -\sigma$. We thus obtain, for the single-site mean-field spin Hamiltonian H_s:

$$H_s = \sum_\sigma h_\sigma \widetilde{O}^\dagger_\sigma + \text{H.c.} + \lambda \sum_\sigma \left(S^z_\sigma + \frac{1}{2}\right), \qquad (B2)$$

with

$$h_\sigma = -\sum_j J_{ij}\langle \widetilde{O}_{j\sigma}\rangle, \qquad (B3)$$

where j indicates the neighbor of site i. Diagonalizing H_s, we obtain the ground state eigenvalue and eigenvector, i.e.,

$$\epsilon_{GS} = \frac{\lambda}{2} - \frac{1}{2}\sqrt{\lambda^2 + 8|a|^2}, \qquad (B4)$$

$$|GS\rangle = \begin{pmatrix} 0 \\ a/N \\ a/N \\ \epsilon_{GS} \end{pmatrix}, \qquad (B5)$$

with

$$N = \sqrt{\epsilon^2_{G.S} + 2|a|^2}. \qquad (B6)$$

Hence, we can determine $\langle S^z_\sigma\rangle$ and $\langle O^\dagger\rangle$.

$$\langle S^z_\sigma\rangle = -\frac{1}{2}\frac{\epsilon^2_{G.S}}{N^2}, $$

$$\langle O^\dagger\rangle = \frac{a^*\epsilon_{G.S}}{\epsilon^2_{GS} + 2|a|^2}(1 + c). \qquad (B7)$$

The Lagrange multiplier is fixed by the constraint equation that depends on the chosen filling:

$$n = \langle S^z\rangle + \frac{1}{2} = \frac{|a|^2}{\epsilon^2_{GS} + 2|a|^2}. \qquad (B8)$$

We can calculate the renormalization factor $Z = |\langle O^\dagger\rangle|^2$ using

$$Z = |\langle O\rangle|^2 = |1 + c|^2\frac{\epsilon^2_{GS}}{|a|^2}n^2 = |1 + c|^2 n(1 - 2n). \qquad (B9)$$

Using the one-band prescription (see Appendix A) $c = \frac{1}{\sqrt{n(1-n)}} - 1$, we then obtain

$$Z = \frac{1 - 2n}{1 - n} = \frac{2x}{1 + x}, \qquad (B10)$$

(where x is the total doping, $2n = 1 - x$). That is precisely the result of the Gutzwiller approximation.

[1] A. Georges, G. Kotliar, W. Krauth, and M. J. Rozenberg, Rev. Mod. Phys. **68**, 13 (1996).

[2] M. H. Hettler, M. Mukherjee, M. Jarrell, and H. R. Krishnamurthy, Phys. Rev. B **61**, 12739 (2000); T. Maier, M. Jarrell, and M. H. Hettler, Rev. Mod. Phys. **77**, 1027 (2005).

[3] G. Kotliar, S. Y. Savrasov, G. Palsson, and G. Biroli, Phys. Rev. Lett. **87**, 186401 (2001).

[4] M. Potthoff, Eur. Phys. J. B **36**, 335 (2003).

[5] Y. M. Vilk and A.-M. S. Tremblay, J. Phys.: Condens. Matter **7**, 1309 (1997).

[6] P. Coleman, Phys. Rev. B **29**, 3035 (1984).

[7] G. Kotliar and A. E. Ruckenstein, Phys. Rev. Lett. **57**, 1362 (1986).

[8] F. Lechermann, A. Georges, G. Kotliar, and O. Parcollet, Phys. Rev. B **76**, 155102 (2007).

[9] S. Florens and A. Georges, Phys. Rev. B **70**, 035114 (2004).

[10] E. Zhao and A. Paramekanti, Phys. Rev. B **76**, 195101 (2007).

[11] S. Florens and A. Georges, Phys. Rev. B **66**, 165111 (2002).

[12] L. de' Medici, A. Georges, and S. Biermann, Phys. Rev. B **72**, 205124 (2005).

[13] P. G. J. van Dongen, Phys. Rev. Lett. **67**, 757 (1991); Phys. Rev. B **49**, 7904 (1994); **54**, 1584 (1996).

[14] R. Pietig, R. Bulla, and S. Blawid, Phys. Rev. Lett. **82**, 4046 (1999).

[15] A. Ochiai, T. Suzuki, and T. Kasuya, J. Phys. Soc. Jpn. **59**, 4129 (1990).

[16] S. Mori, C. H. Chen, and S.-W. Cheong, Nature (London) **392**, 473 (1998); C. H. Chen and S.-W. Cheong, Phys. Rev. Lett. **76**, 4042 (1996).

[17] Y. Tomioka, A. Asamitsu, H. Kuwahara, and Y. Tokura, J. Phys. Soc. Jpn. **66**, 302 (1997).

[18] Ping Sun and G. Kotliar, Phys. Rev. B **66**, 085120 (2002).

[19] C. J. Bolech, S. S. Kancharla, and G. Kotliar, Phys. Rev. B **67**, 075110 (2003).

[20] Hiroshi Watanabe and Masao Ogata, J. Phys. Soc. Jpn. **74**, 2901 (2005).

[21] B. Davoudi, S. R. Hassan, and A.-M. S. Tremblay, Phys. Rev. B **77**, 214408 (2008).

[22] O. I. Motrunich and P. A. Lee, Phys. Rev. B **69**, 214516 (2004).

[23] O. I. Motrunich and P. A. Lee, Phys. Rev. B **70**, 024514 (2004).

[24] G. Baskaran, Phys. Rev. Lett. **91**, 097003 (2003).

[25] B. Kumar and B. S. Shastry, Phys. Rev. B **68**, 104508 (2003).

[26] Q.-H. Wang, D.-H. Lee, and P. A. Lee, Phys. Rev. B **69**, 092504 (2004).

[27] Weihong Zheng, Jaan Oitmaa, Chris J. Hamer, and Rajiv R. P. Singh, Phys. Rev. B **70**, 020504(R) (2004).

[28] S. R. Hassan, L. de' Medici, and A.-M. S. Tremblay, Phys. Rev. B **76**, 144420 (2007).

[29] It is worth noting that the auxiliary spin has nothing to do with the physical spin, that is treated here just as a label. In fact a

slave-spin variable is introduced for every fermion species, taking into account the fermion spin multiplicity, so that slave-spins are also labeled with a spin index, i.e., $S^z_{i\sigma}$.

[30] When $c_{i\sigma}$ is not of unit modulus, there is no problem with anticommutation relations, if they are taken between physical states.

[31] J. Merino, B. J. Powell, and R. H. McKenzie, Phys. Rev. B **73**, 235107 (2006).

[32] M. Capone, L. Capriotti, F. Becca, and S. Caprara, Phys. Rev. B **63**, 085104 (2001).

[33] B. Kyung, Phys. Rev. B **75**, 033102 (2007).

[34] A. H. Nevidomskyy, C. Scheiber, D. Sénéchal, and A.-M. S. Tremblay, Phys. Rev. B **77**, 064427 (2008).

[35] F. C. Chou, J. H. Cho, P. A. Lee, E. T. Abel, K. Matan, and Y. S. Lee, Phys. Rev. Lett. **92**, 157004 (2004).

[36] D. J. Singh, Phys. Rev. B **61**, 13397 (2000).

[37] L. de' Medici, S. R. Hassan, M. Capone, and X. Dai, Phys. Rev. Lett. **102**, 126401 (2009).

[38] L. de' Medici, Ph.D. thesis, Ecole Polytechnique and Université de Paris-Sud, 2006.